

USING ANTENNAE FOR IN-SITU MEASUREMENTS OF MICROMETEOROID AND SPACE DEBRIS IMPACTS

Martin Schimmerohn⁽¹⁾, Max Gulde⁽¹⁾, Alain Hilgers⁽²⁾

⁽¹⁾Fraunhofer-Institute for High-Speed Dynamics, Ernst-Mach-Institut, EMI, Eckerstr.4, 79104 Freiburg, Germany, Email: martin.schimmerohn@emi.fraunhofer.de, max.gulde@emi.fraunhofer.de,

⁽²⁾ESA/ESTEC, Keplerlaan 1, Postbus 299, 2200 AG Noordwijk, The Netherlands, Email: alain.hilgers@esa.int

ABSTRACT

The hypervelocity impact of micrometeoroids and space debris produce a transient plasma cloud when colliding with spacecraft surfaces. We studied the feasibility of using the interactions between the fast expanding impact plasma clouds with spacecraft antennae for in-situ impact detection. We used a numerical model for computing the formation and evolution of the plasma cloud as well as the signals generated at the antenna sensors. The generation of secondary electrons at the antennae due to fast ions in the plasma cloud proved to be an effective mechanism to correlate sensor signals to impactor characteristics. We demonstrated that a simple array of seven centimeter-sized antennae is sufficient to trace back impactor size and impact velocity.

1 INTRODUCTION

Mechanical effects like cratering, perforation and fragmentations are the most obvious consequences of the hypervelocity impact of meteoroids and space debris. However, the first and most direct effect of a hypervelocity collision is the fast expansion of a plasma cloud from the impact location, referred to as impact plasma. It consists of vaporized and ionized material from both impactor and the impacted component.

The impact plasma shows a range of distinct plasma phenomena that can be exploited to detect impacts and to deduce its initial conditions. Such effects include the presence of free charges and the emittance of electromagnetic waves. From the 1960s, dedicated laboratory diagnostics have been developed to exploit both effects for characterizing hypervelocity impacts, in particular for impacts of sub-micron sized impactors as simulated using electrostatic accelerators [1], [2]. This led to a heritage of space-born dust detectors, which are based on the electrostatic extraction of free charge carriers of impact plasma clouds that are generated by impacts inside a screened vessel [3], [4], [5]. These detectors are complex instruments and mainly motivated by investigating the chemical composition of micrometeoroids on interplanetary missions.

Concurrently, impact plasma effects have also been detected unexpectedly by radio and plasma wave instruments on-board several spacecraft. Noise signals

showing up as voltage spikes have been attributed to interactions of the expanding impact plasma cloud with the antennae of the space plasma diagnostics. Fig. 2 shows an example of such signals measured with the WAVE instrument on-board the STEREO-A spacecraft, while its identical counterpart STEREO-B monitors the same plasma environment but no such noise signals [6].

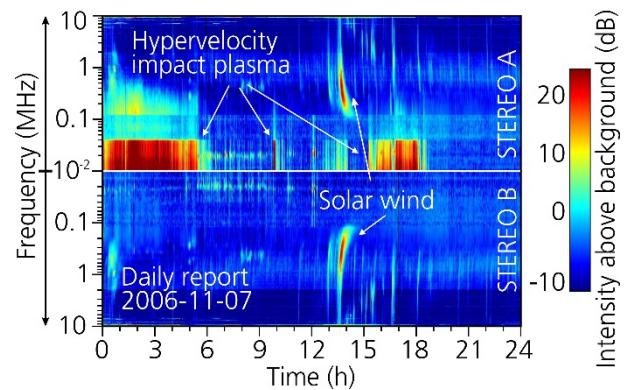


Figure 1. STEREO A/B spectrograms adapted from [7]

Those observations gave rise to controversy about the mechanisms of signal generation but also triggered the question whether this effect can be applied for impact detection. In this context, we have studied the feasibility of using antennae on spacecraft surface as an in-situ impact diagnostic [8]. Three fundamental questions have been addressed:

- 1) How do the characteristics of the impact plasma cloud correlate with the impact conditions over a broad parameter range?
- 2) How do the generated antenna signals correlate with the characteristics of the impact plasma cloud?
- 3) What does a suitable detector concept look like?

2 IMPACT PLASMA

The generation of plasma is comprehensible in view of the extreme pressure and temperature conditions at the interface of two objects colliding in the hypervelocity range. Shock fronts are initiated and travel through the particle and target from the collision interface. The material's internal energy behind the shock front is raised and dissipated as an increase in both entropy and

temperature. Reached temperatures in excess of 10^5 K are sufficient to cause vaporization and ionization of shocked material during relaxation from the shock state. As soon as a shock front reaches a free surface, the ionized gas is released and expands into the vacuum, thus forming the transient impact plasma cloud.

Fig. 2 shows the expansion of an impact plasma cloud in experiment. It is a combination of high-speed images in pseudo-colour at five different times after impact. The size and velocity of the impactor, a 3 mm diameter aluminum sphere impacting under 45° with 7 km/s on an aluminum target, are indicated.

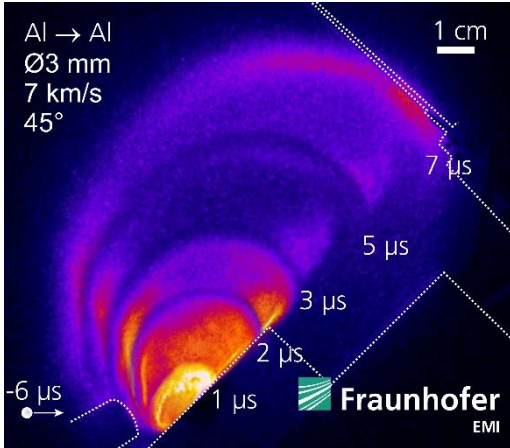


Figure 2. Plasma expansion observed in experiment

The image shows the plasma cloud propagating along the impacted surface. The light emissions weaken as the temperature and density rapidly decrease during expansion [9]. After seven microseconds, the optically thin cloud shows intensity increase at its boundary, where it starts to interact with a metallic rod.

Such experiments give important insight in plasma cloud characteristics. However, impact plasma investigations are complicated by their small size, high energy density and transience. Therefore, the detector study was based on simulations to allow for a wide parameter range that is not completely accessible through ground experiments.

2.1 Impact plasma modelling

We developed a comprehensive impact plasma model for quantitatively describing the spatial and temporal evolution of the impact plasma cloud as a function of impact parameters. We adapted the method by Drapatz and Michel [10] and combined it with approaches from different scientific/technical fields of application. Those fields include impact physics (shock state and impact vaporization), astrophysics (properties and ionization of a gas mixture under high pressure), and laser physics (plasma expansion). Where applicable, we used semi-empirical approaches to limit the computational effort for the parametric study. The complete model will be

described in another publication [8].

Its nominal theory is the thermal volume ionization. Strong shock waves dissociate and ionize material when propagating through impactor and target material. We applied the planar impact approximation and a semi-empirical equation of state to determine the shock state characteristics. The amount of vaporized materials follows from the entropy method under consideration of empirical laws of shock pressure decay. The initially extremely dense cloud is in Saha equilibrium with mixture concentrations of ion species calculated accordingly as shown in Fig. 3. It shows the decrease of ionization due to the cooling and thinning during expansion of a plasma cloud resulting from a $100 \mu\text{m}$ Al particle hitting a quartz surface with at 25 km/s

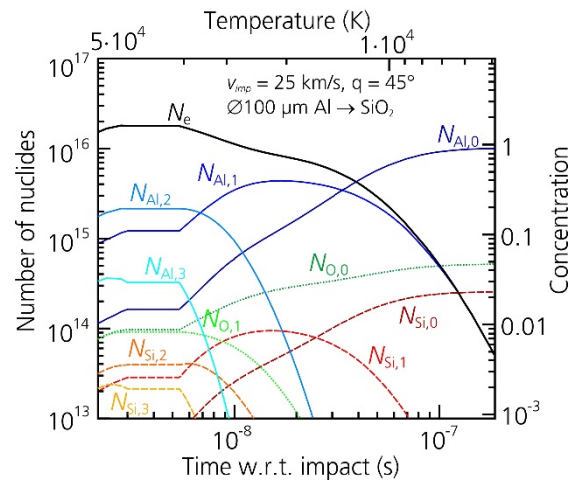


Figure 3. Equilibrium plasma composition

At some point during expansion, the thinning cloud goes into a phase of non-equilibrium recombination, during which the degree of ionization drops rapidly. Under certain circumstances, if/when the mean free path of electrons grows larger than the cloud size, the plasma cloud becomes collisionless and charge separation effectively takes place at the cloud boundary. We consider both scenarios by applying self-similar models with linear velocity distribution [11], [12] for all expansion phases of the impact plasma cloud.

The resulting model uncertainties are at a similar level as the input conditions. These stem from the lack of material data for extreme compressions and the unknown particle characteristics, particularly their density and shape. The model uncertainties, however, are higher for lower impact velocities, i.e., for $v < 20$ km/s for most of solid materials. At these velocities, the above described mechanism of volume ionization under the effect of strong shock waves is not dominant anymore but outnumbered by different surface ionization processes. As no applicable quantitative model for the surface ionization exist, we treat this velocity regime like an initial value problem that uses

the volume ionization routine for simulation and available empirical charge yield relations as boundary condition. Those charge yield relations originate from ground measurements using electrostatic extraction. Extending impact experiments with focus on plasma measurements would improve the accuracy of the model in the velocity regime <20 km/s.

2.2 Plasma cloud characteristics

We applied the impact plasma model in a parametric study to investigate correlations between the characteristics of the impact plasma cloud with the impact parameter, i.e. particle size as well as impact velocity and angle. We simulated impactors in the size range of $0.1 \mu\text{m}$ to $100 \mu\text{m}$ and impact velocities between 2 km/s and 100 km/s. The studied materials of impactor and impacted component are silicon dioxide, aluminum, iron and gold.

We found no pronounced influence of the studied material combinations. This means that antenna based impact detection is not an appropriate method to investigate the chemical composition of impactors. However, the weak dependency on materials enables a significant correlation of cloud density on particle size and velocity. Fig.4 shows the electron density of impact plasma clouds generated by oblique SiO_2 -Au-impacts as a function of impactor size and velocity. The plasma clouds have expanded to 20 cm size. The white contour plots represent typical impact fluxes according to the Grün model with Taylor velocity distribution, to illustrate the probability of parameter combinations.

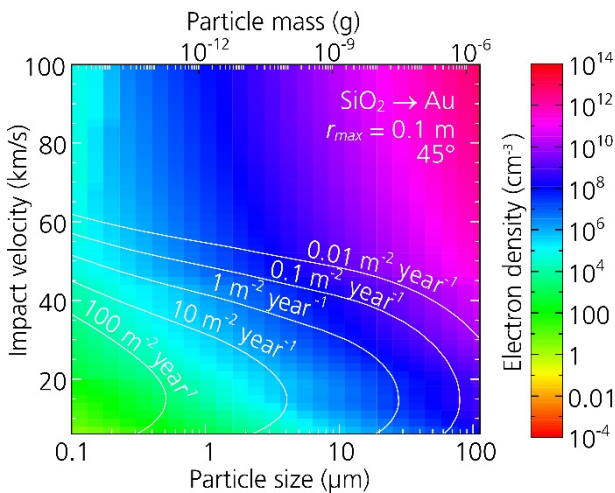


Figure 4. Electron density vs. particle mass and velocity

The relative density distribution in the size-velocity parameter space is maintained during cloud expansion. This is due to a direct correlation between impact velocity and cloud expansion velocity that is notably independent from the particle size within a wide range: the impact velocity determines the amount of dissipated thermal energy that drives the expansion velocity of the

generated plasma cloud. Besides a thermally driven radial component, the impact plasma expansion has a horizontal component that retains part of the impact directionality due to shock geometry in oblique impacts. This can be observed as an upward directed movement of the plasma cloud in Fig.2.

There exists an exception for very small and very fast particles. They generate a very fast expanding plasma that falls earlier off equilibrium, thus maintaining a higher ionization and becoming collisionless during expansion. However, in our simulation we found collisionless plasma clouds only for a limited range of parameters, i.e., for sub-micron particles.

3 SENSOR SIGNALS

We identified a number of direct correlations between the plasma cloud density and its expansion with the particle size, velocity and impact angle. Now we discuss the responses of antennae interacting with the cloud. In doing so, the used term antenna might be misleading, as we do not measure radio signals, but a direct change of the antenna charge equilibrium.

3.1 Sensor response modelling

In the model, the evolving plasma cloud expands over the spacecraft surface, thereby covering an antenna that is located in a specific distance and orientation with respect to the impact location. Fig. 5 illustrates the scenario for exemplary values of impact parameters (green) and sensor parameters (blue) at five time steps.

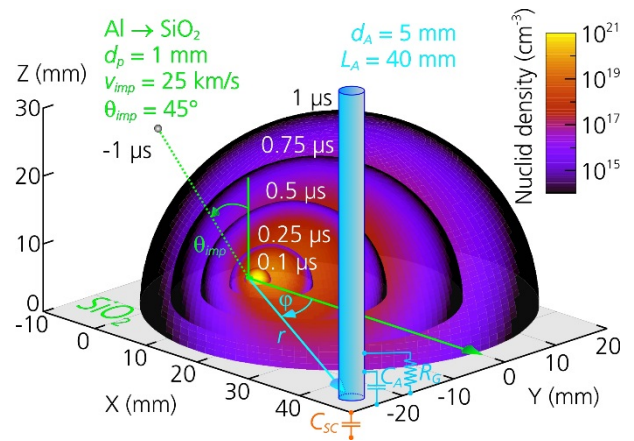


Figure 5. Simulation of impact plasma cloud and sensor

The potential of the antenna is disturbed through the free charge carriers in the plasma cloud. This happens on a timescale shorter than needed for equilibrium establishment with plasma currents from the spacecraft environment. We consider four mechanisms to cause a measurable effect at the passive antenna:

- 1) The direct detection of free charges at the antenna surface covered by the impact plasma. Only the net-sum of charge is detected. Therefore, signals are

generated in case the cloud has become collisionless and charge separation has taken place, or cloud electrons are re-collected by the spacecraft potential.

- 2) The collection of cloud charge carriers by the charged spacecraft surface. This causes a change of the spacecraft potential with respect to the antenna. Thus, contrary to the other signal generation mechanisms, it is independent of direct interactions of antenna and plasma cloud [13].
- 3) The disturbance of the antenna potential by blocking the photoelectron return current in the impact plasma cloud, as proposed by Pantellini [14].
- 4) The disturbance of the antenna potential by emission of secondary electrons through the primary particle flux of ions in the fast expanding plasma cloud.

The last mechanism was so far unconsidered in the discussions about the generation of noise signals on spacecraft. However, we observe such effects in experiments as for example shown in Fig.2 for the last time step. The very high and directed expansion velocity of the ions with respect to the antenna explains the emission of secondary electrons.

We expanded the impact plasma model by these effects. Besides antenna position and dimension, the spacecraft potential need to be included. We assumed a constant spacecraft potential as the impact plasma expansion occurs on a shorter time scale than the establishment of electrostatic potential equilibrium.

3.2 Signal characteristics

We found that the emission of secondary electrons (4) and the re-collection of cloud electrons by the spacecraft potential (2) results in exploitable signals. As Fig.6 shows, both induce exploitable signal intensities.

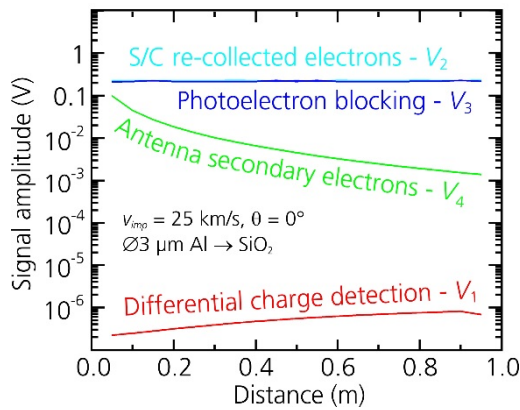


Figure 6. Detectable voltage levels

The diagram shows the absolute detectable voltages for the different detection mechanisms as a function of distance between impact site and antenna base for a small impactor. The detected voltage amplitudes resulting from the direct detection of cloud electrons (1)

are too low for exploitation. This is due to the quasi-neutrality of the plasma cloud for large impactor. Sub-micron sized impactors generate collisionless clouds with a separated electron front; however, their absolute number of charge carriers is quite low.

The recollection of electrons yields high amplitudes (as a function of spacecraft charging conditions) but is independent of the direct plasma cloud interactions. This effect may provide an additional reference for data exploitation.

The disturbance of the photoelectron return current yields high amplitudes but is not considered as it is 1) too sensitive to Sun illumination and 2) the mechanism still needs to be characterized in experiments.

The so far unconsidered secondary electron emission by the fast ions in the cloud proved to be an exploitable effect. The signals have both measurable amplitudes and direct dependencies to cloud characteristics and antenna position. This is demonstrated in Fig.7, which shows the characteristic signal rise time as a function of antenna position in polar coordinates for the impact of a 2 μm particle hitting on a SiO_2 surface at 25 km/s und 30°.

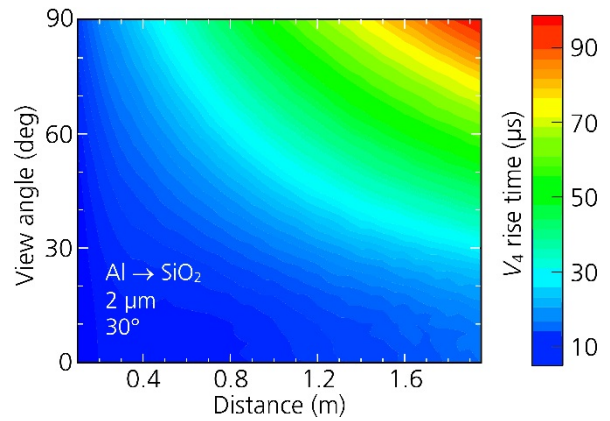


Figure 7. V_4 Signal rise time vs. antenna position

A typical waveform for impact plasma induced electron emission is shown in Fig. 8 (bottom panel). The rise time is a result of the cloud-antenna interactions. The decay time is a function of the time needed for the recovery of the initial spacecraft charging conditions.

The characteristic times increase with antenna distance, because the cloud density profile is maintained during expansion, ultimately leading to longer propagation times at the antenna. For oblique impacts, the time constants also become dependent on the angle of detection due to the horizontal velocity component. The strong dependence of the time constants on the horizontal velocity component will render an analysis of the signals waveform important for the determination of impact parameter. It is apparent that an array of antennae is needed to extract information of the impact parameters from measured signals.

4 DETECTION CONCEPT

We simulated exemplary cases for different antenna arrays to check the feasibility of the detection concept and to find an optimum configuration. Fig.8 shows such a configuration. It consists of a hexagonal array of seven unbiased antennae of 30 cm length and 1 cm diameter with 30 cm spacing between the antennae.

We simulated the induced responses of each antenna and demonstrated that information on the impact can be derived from the multiple signals. We recovered the impact parameters by using triangulation and simple analytical fit functions for the simulated sensor signals. Using this simple sensor configuration, we can efficiently trace back the most important impact parameters with good accuracy.

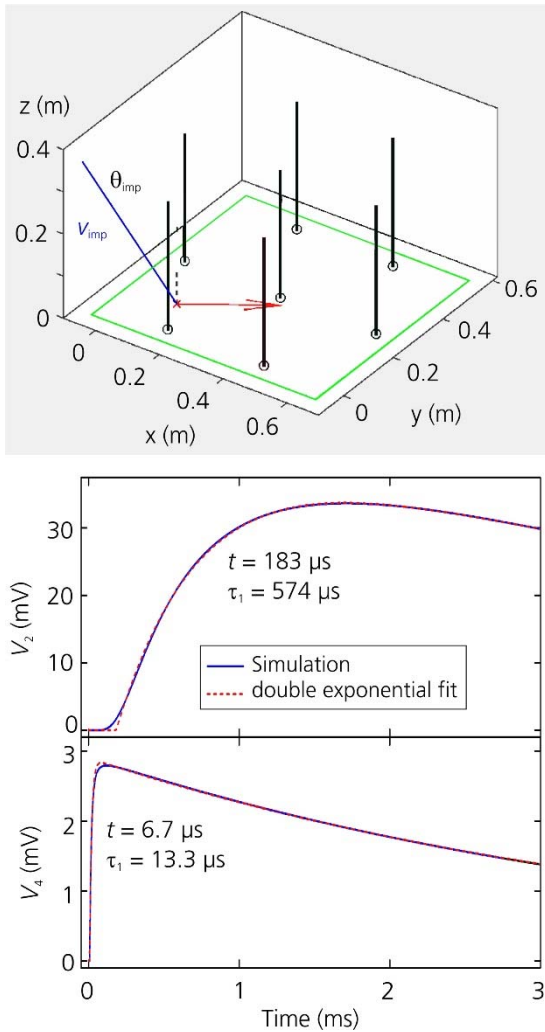


Figure 8. Detector concept and impact signatures

In the shown example, we determined the impact location and velocity with less than 5 % deviation. The impact angle and the particle mass were sampled with <15 % deviation.

4.1 Instrument requirements

Based on the findings and analysis results, we derived the following instrument requirements:

- 1) A sensor shall consist of an array of a minimum of six orthogonal antennae with equidistant positioning and a grid spacing of ca. 30 cm.
- 2) Each antenna has a length of ca. 30 cm and a diameter of 1 cm to 2 cm. We consider standard values for spacecraft monopoles for the antenna wiring. The sensors are passive (i.e., not biased).
- 3) The detection surface shall be made of a plane layer from homogeneous material with a minimum thickness of 1 mm.
- 4) The antennae need to be sampled with a minimum time resolution of 0.1 μ s.
- 5) The minimum signal resolution shall be better than 0.01 mV. The maximum amplitude is 5 V.

The impact detection system shall also include an instrument for in-situ monitoring of the surface charge at the detection surface. We consider a combination with a compact state-of-the-art, flight-proven charge detector for this purpose. As it is true for all impact detection methods, additional impact detecting instruments would improve the sensor performance by providing an independent reference. Without going into details of other impact detection methods, we generally recommend the use of a complementary and coincident measurement of particle impacts.

4.2 Development roadmap

The striking benefit of the studied detection concept is its simplicity. The sensor itself, as indicated above, has a quite simple design and the data processing is feasible with standard FPGA-based electronics. Arbitrary spacecraft surfaces may be used for detection.

Dedicated activities are needed to experimentally verify the detection concept and to systematically study impact plasma characteristics. Impact induced charge emissions and the expected signal responses at centimeter-sized antennae can be studied in hypervelocity impact ground experiments for different particle sizes and impact conditions. In addition, the antenna-spacecraft charging under the influence of transient impact plasma should be studied numerically to assess the signal noise levels.

5 CONCLUSIONS

We studied the feasibility of an in-situ impact detector that is based on impact plasma signatures measured by antennae. We developed and applied a comprehensive model to simulate the formation, the expansion, and the interaction of impact induced plasma clouds with antennae in a broad impact parameter range. We

demonstrated that, in principle, a simple array of six centimetre-sized antennae is sufficient to trace back basic impact parameters such as particle size, impact angle, and impact velocity with reasonable accuracy. Its simple design is the primary advantage of this concept for in-situ impact detection. Once the concept is verified in dedicated ground experiments and numerical simulations of antenna noise signals, it may be realized using state-of-the-art technology.

ACKNOWLEDGEMENT

This work was funded by the European Space Agency under contract 4000107623/13/NL/AF in the general studies programme.

REFERENCES

1. Friichtenicht, J.F., Slattery, J.C. (1963). *Ionization associated with Hypervelocity Impact*. NASA TN D-2091
2. Jean, B., Rollins, T.L. (1970). Radiation from Hypervelocity Impact generated Plasma. *AIAA Journal* 8 (10), 1742-1748.
3. Dietzel, H., Eichhorn, G., Fechtig, H. et al. (1973). The HEOS 2 and HELIOS Micrometeoroid Experiments. *J. Phys. E – Sci. Instr.* 6, 209-217.
4. Göller, J.R., Grün, E. & Maas, D. (1987). Calibration of the DIDSY-IPM Dust Detector and Application to other Impact Ionisation Detectors on board the P/Halley Probes. *Astron. Astrophys.* 187, 693-698.
5. Srama, R., Ahrens, T.J., Altobelli, N. et al. (2004). The CASSINI Cosmic Dust Analyzer. *Space Sci. Rev.* 114, 465-518.
6. Meyer-Vernet, N. & Zaslavsky, A. (2012). In Situ Detection of Interplanetary and Jovian Nanodust with Radio and Plasma Wave Instruments. In *Nanodust in the solar system: discoveries and interpretations* (Eds. I. Mann et al.), Springer, 133-160.
7. Kaiser, M. (2013). Data Plots for STEREO-WAVES and other Instruments. <http://swaves.gsfc.nasa.gov/cgi-bin/wimp.p>.
8. Schimmerohn, M. (2015). *Detection of Microparticle Impacts on Spacecraft via their Plasma Effects*. Final Report ESA contract 4000107623/13/NL/AF, Fraunhofer EMI report I-50/15, Oktober 2015.
9. Heunoske, D., Schimmerohn, M., Osterholz, J., Schäfer, F. (2013). Time-resolved Emission Spectroscopy of Impact Plasma. *Procedia Engineering* 58, 624-633.
10. Drapatz, S. & Michel, K.W. (1974). Theory of Shock-Wave Ionization upon High-Velocity Impact of Micrometeorites. *Z. Naturforsch. A)* 29, 870-879.
11. Anisimov, S.I., Luk'yanchuk, B.S. & Luches, A. (1995). Dynamics of the three-dimensional expansion in a vapor produced by a laser pulse. *JETP* 81(1), 129-138.
12. Murakami, M. & Basko, M.M. (2006). Self-similar Expansion of finite-size non-quasi-neutral Plasmas into Vacuum: Relation to the Problem of Ion Acceleration. *Phys. Plasmas* 13, 012105.
13. Oberc, P. (1996). Electric Antenna as a Dust Detector. *Adv. Space Res.* 17(12), 105-110.
14. Pantellini F, Belheouane, S., Meyer-Vernet, N. & Zaslavsky, A. (2012). Nano Dust Impacts on Spacecraft and Boom Antenna Charging. *Astrophys. Space Sci.* 341, 309–314.